Strictly hyperbolic models of co-current three-phase flow with gravity

Ruben Juanes
Tadeusz W. Patzek

Department of Civil and Environmental Engineering
University of California at Berkeley
631 Davis Hall #1710, Berkeley, CA 94720

Earth Sciences Division
Lawrence Berkeley National Lab
1 Cyclotron Road Mailstop 90–1116, Berkeley, CA 94720

Submitted to *Transport in Porous Media*

November 18, 2002

Abstract

We study the character of the equations in the traditional formulation of one-dimensional immiscible three-phase flow with gravity, in the limit of negligible capillarity. We restrict our analysis to co-current flow required for a *displacement* process; in cases of mixed co-current and counter-current flow, capillarity effects cannot be dropped from the formulation. The model makes use of the classical multiphase extension of Darcy's equation. It is well known that, if relative permeabilities are taken as fixed functions of saturations, the model yields regions in the saturation space where the system of equations is locally elliptic. We regard elliptic behavior as a nonphysical artifact of an incomplete formulation, and derive conditions on the relative

permeabilities that ensure strict hyperbolicity of the governing equations. The key point is to acknowledge that a Darcy-type formulation is insufficient to capture all the physics of three-phase flow and that, consequently, the relative permeabilities are *functionals* that depend on the fluid viscosity ratio and the gravity number. The derived conditions are consistent with the type of displacements that take place in porous media. By means of an illustrative example, we show how elliptic behavior can be removed, even when using simplistic relative permeability models.

KEY WORDS: porous media, three-phase flow, gravity, relative permeability, strict hyperbolicity, elliptic regions

1 Introduction

Mathematical models of multiphase flow in porous media have been developed, to a large extent, by extension of models that were successful in modeling flow of a single fluid. This is particularly true for three-phase flow, which has been traditionally modeled using a direct application of two-phase flow formulations [9, 15, 45, 47] (see also [44] and the references therein). As it turns out, three-phase flow is less forgiving than two-phase flow, and exposes the physical and mathematical inconsistencies of the classical approach. In our opinion, the use of the simple classical approach has been favored by two factors: first, the limited understanding of the physics of flow of several phases in a porous medium; and second, the challenge of posing the mathematical problem in a tractable form that allows the development of predictive tools.

The importance of two-phase flow in porous media has long been recognized in many fields [12, 14, 46, 50]. Although investigated from the very onset [41,45], the need for quantitative predictions involving flow of *three* fluid phases is more recent. However, there is now little doubt that a good description of three-phase flow is essential in practical applications like enhanced oil recovery [16, 36, 38, 48] and environmental remediation of the unsaturated zone [1–3, 19, 20].

1.1 Scaling of the multiphase flow equations

One of the main difficulties in the mathematical modeling of multiphase flow is its inherent multiscale character. In fact, we regard multiphase flow not only as a multiscale problem —where the parameters and the variables of interest are scale-dependent, but also a multiphysics problem —different *processes* dominate at different scales: the microscale is controlled by capillary forces, whereas viscous and gravity forces seem to dominate at the macroscale. In traditional scaling of the multiphase flow equations, the effects of capillarity scale as the inverse of the length of the domain [22, 49]. As a result, capillarity effects are sometimes dropped from the field-scale equations. This is sensible only if the solutions with capillarity converge to the capillarity-free solution as the capillarity effects are taken to zero. In the context of multiphase displacements, capillarity effects lead to a nonlinear diffusion term in the macroscopic continuum conservation equations [15]. Here, the role of capillarity is to smear the moving fronts that arise from the displacement of one fluid by another.[1] As capillarity effects vanish, one expects that the solution to the macroscopic equations will develop sharp features, such as shocks and boundary layers. At a smaller scale, however, there is a transition zone where a drastic change of saturations occur. Depending on the pore-scale displacement mechanisms, this transition zone will be more or less abrupt. Indeed, the behavior of the transition zones may vary wildly, and may depend on the wettability properties of the fluids, the fluid viscosity ratios, the fluid density ratios, the displacement process —drainage or imbibition—, and the displacement history that determined the pore-scale configuration of the fluids [4,5,39,40]. To properly account for the physics of multiphase flow, it is likely that one has to resort to a multiscale formulation. The development of such a formulation still is an open issue and, although several approaches have been proposed [6, 11, 23, 27, 54, 58], they yet have to be fully explored.

1.2 Darcy's equation

Traditional formulations of multiphase flow describe macroscopic fluid fluxes with a straightforward extension —first proposed by Muskat [45]— of Darcy's

[1] The term "smeared front" is referred to as "viscous profile" in the field of fluid mechanics. We have avoided this terminology because the shape of fronts in multiphase displacements is governed by capillary forces, not viscous forces!

equation for single-phase flow. It is well known that, unlike in the single-phase case [26], this extension cannot be rigorously obtained from first principles [28]. The multiphase extension of Darcy's equation may be described as a quasi-linear relation, because the fluid flux depends linearly on the "driving force" —which includes viscous, capillary, and gravity forces— and all the nonlinearity is agglutinated in the relative permeabilities.

Darcy-type models do not reflect any of the small-scale considerations described above. The only way in which they can capture at least a shadow of the behavior of the actual displacement is through the relative permeability functions, because these are the only "degrees of freedom" of the formulation. Therefore, relative permeabilities cannot be understood as fixed functions of saturation, or even saturation history. The depend intrinsically on the flow regime and properly should be called *functionals* rather than functions. This is certainly not an ideal description. The very presence of functionals is a reflection of having an *incomplete* formulation [10, 28].

In this paper we make use of the multiphase extension of Darcy's equation as a *working assumption*, rather than a physical law. In this context, we regard the relative permeability as nothing else than a *functional* used in the constitutive model, which may —and in fact *should*— be influenced by the fluid viscosity ratios and the gravity number. It is precisely the influence of viscosity and gravity on the relative permeabilities that allows one to remove some of the mathematical inconsistencies of the classical formulation of three-phase flow.

1.3 Character of the equations

When the fractional flow formalism is used, flow through porous media of three immiscible, incompressible fluids is described by a pressure equation —whose solution is trivial in the one-dimensional case— and a 2×2 system of saturation equations [15, 47]. It was first shown in [13] that certain relative permeabilities would yield a system of equations that was not strictly hyperbolic for all saturation states. Indeed, regions in the saturation triangle where the system is locally elliptic —the so-called elliptic regions— are present for most relative permeability functions used today [13, 21, 32, 34, 52, 53]. The only models that do not display elliptic regions are those where the relative permeability of each phase is a function of its own saturation only [43, 57]. In this case, elliptic regions shrink to isolated umbilic points, where eigenvalues of different families are equal.

The analysis of Shearer [52] and Holden [32] suggests that elliptic regions are an unavoidable consequence of three-phase flow models. This important result has had two consequences: (1) further investigation on the theory of conservation laws for mixed elliptic/hyperbolic systems (see, *e.g.*, the monographs [37, 42] and the references therein); and (2) a widespread controversy about whether elliptic regions are physical [33]. As for (1), although a few qualitative aspects are known [29–31], a complete mathematical theory of mixed elliptic/hyperbolic systems is still lacking. In particular, correct entropy conditions —needed to remove nonuniqueness of the solutions— are not yet known [7,8]. As for (2), we think that the presence of elliptic regions should *not* be justified simply because they appear in a Darcy-type formulation of three-phase flow with relative permeability that are fixed functions of saturations.[2] In particular, the analysis in [32, 52] *assumes* a particular behavior of the relative permeabilities on the edges of the saturation triangle.

In a previous paper [35], we argued that the system describing three-phase *displacements* should be strictly hyperbolic, and we identified conditions on the relative permeabilities so that this essential feature is preserved. The generic conditions that need to be imposed on the relative permeability functions seem to be in agreement with experimental observations and pore-scale physics. We now extend the previous analysis to incorporate gravity effects.

1.4 Effects of gravity

When gravity is included in the analysis, it was shown that a large class of models of three-phase relative permeabilities may yield elliptic regions [57]. The effect of gravity on elliptic regions has also been illustrated elsewhere [24, 33,34,53]. In all these investigations, the usual extension of Darcy's equation to multiphase flow is adopted without further discussion. In addition, relative permeabilities are taken as fixed functions of saturations, independent of the flow regime. Ellipticity of the equations arises because the "driving force" is modified by including a dominant gravity term, while the relative permeability functions are kept unchanged.

In [35] we conjectured that relative permeabilities would vary in such a way that the system of equations —including the gravity term— would remain everywhere strictly hyperbolic. In this paper we conclude that, under

[2] We agree completely with Shearer and Trangenstein [53], when they say that "We have no reason to believe that the elliptic regions are physical; rather, we believe that they are an unintended consequence of the forms of the three-phase flow models."

certain *physical* conditions, our conjecture was correct. An essential feature of our study is that we restrict the analysis to *displacement* processes, where the role of capillarity effects is simply to smear out the moving fronts. Physically, we are limited to systems with *co-current flow* for all saturation states. In situations with mixed co-current and counter-current flow, the effect of capillarity *cannot* be neglected. In those situations, the capillarity-free model is no longer valid.

To avoid misunderstanding, we want to distinguish our approach from that of other investigations, such as those of Trangenstein [57], and Jackson and Blunt [33]. Trangenstein [57] neglects any potential dependence of the relative permeabilities on the flow regime, and he states this assumption explicitly: "... I will assume that the relative permeabilities are only allowed to depend on the phase saturations. Thus, given the relative permeability functions, it will be fair game to vary the viscosities, mass densities, total fluid velocity and reservoir dip angle in order to obtain complex characteristic speeds." In view of our observations above, this assumption is not realistic, because the presence of gravity modifies pore-scale displacements which, in turn, yield different macroscopic relative permeabilities.

Similarly, Jackson and Blunt [33] assume that relative permeabilities are fixed functions of fluid saturations alone, and evaluate the character of the system for large values of the gravity number. Their values are well outside the range yielding co-current flow. Our analysis does not apply to the mixed co-current/counter-current conditions they encounter. In fact, and this is partly what they observe, we think that in such cases capillarity cannot be dropped from the formulation. Jackson and Blunt [33] take a unique step in justifying elliptic regions as physically plausible. They use a serial model of capillary bundles to demonstrate that elliptic regions exist in a simplistic but physically realizable porous medium. However, a three-phase displacement process in a sequence of bundles *cannot* be described in the form proposed by the authors. The constraints imposed by the fractional flow formalism and by the proposed communication between bundles reduce their model to a *single* bundle of capillary tubes. The latter model is inappropriate in the context of a displacement process described by the volume-averaged mass and momentum balances dominated by viscous and gravity forces. Therefore, the relative permeabilities used in [33] should be understood as another empirical model. The presence of elliptic regions in Jackson and Blunt's *model* does not imply that they exist in *reality*.

1.5 Paper outline

Here we derive conditions the relative permeabilities must satisfy for the system of saturation equations to be strictly hyperbolic, when gravity is included in the formulation. The crucial point is to acknowledge that, because a Darcy-like formulation is incomplete, the relative permeability functions may depend on the fluid viscosity ratios and on the gravity number. It is reasonable to think that the effect of gravity and viscosity ratios will be most pronounced in the relative permeability to gas, which is usually the least wetting, the least viscous, and the least dense fluid phase. By means of an illustrative example, we show that this dependence may not be strong, but sufficient to remove elliptic behavior. The required conditions for strict hyperbolicity, which are derived from strictly mathematical arguments, are then analyzed from a physical viewpoint. It is found that they are consistent with, and may justified from, the observed behavior of fluid displacements that take place in porous media.

This paper is organized as follows. In Section 2, we present the traditional mathematical formulation of one-dimensional, immiscible three-phase flow, which makes use of the common multiphase extension of Darcy's equation. We express the resulting system of equations in dimensionless form and discuss its mathematical character. In Section 3, we derive conditions for strict hyperbolicity of the system, and show they are closely-related to the conditions for co-current flow. These conditions are then examined from a physical viewpoint. In Section 4, we give an example of how to accommodate the abstract conditions for strict hyperbolicity for a particularly simple relative permeability model, and illustrate the effects of removing elliptic behavior. Finally, in Section 5, we summarize the main conclusions and recommendations.

2 Mathematical formulation

2.1 Mass conservation equations

We study one-dimensional flow of three immiscible, incompressible fluids, through a rigid and homogeneous porous medium. We shall denote the fluid phases as water (w), oil (o), and gas (g). The mass conservation equation

corresponding to the α-phase is, in the absence of source terms:

$$\partial_t m_\alpha + \partial_x F_\alpha = 0, \qquad 0 < x < L,\ t > 0, \qquad \alpha = w, o, g\,, \tag{1}$$

where m_α is the mass of the α-phase per unit bulk volume, F_α is the mass flux of the α-phase, $\partial_t(\cdot)$, $\partial_x(\cdot)$, denote partial derivatives with respect to time and space, respectively, and L is the length of the domain. The mass of the α-phase per unit bulk volume is:

$$m_\alpha = \rho_\alpha S_\alpha \phi, \tag{2}$$

where ρ_α is the density of the α-phase, S_α is the saturation of the α-phase, and ϕ is the porosity. Because the fluids and the medium are assumed to be incompressible, the phase densities and the porosity are constant. The mass flux of the α-phase takes the form:

$$F_\alpha = \rho_\alpha v_\alpha \phi, \tag{3}$$

where v_α is the velocity of the α-phase. A major assumption in the traditional theory of multiphase flow is the use of Muskat's extension [45] of Darcy's equation to model the fluid velocities. If capillarity effects are not included in the formulation, the fluid velocity of the α-phase is modeled by:

$$v_\alpha = -\frac{k}{\phi}\frac{k_{r\alpha}}{\mu_\alpha}(\partial_x p + \rho_\alpha g \partial_x z), \tag{4}$$

where k is the absolute permeability, $k_{r\alpha}$ and μ_α are the relative permeability and the dynamic viscosity of the α-phase, respectively, p is the pressure, common to all phases, g is the gravitational acceleration, and z is the elevation. To simplify notation, we define $g_x := g\partial_x z$. We also define the relative mobility of the α-phase as

$$\lambda_\alpha := \frac{k_{r\alpha}}{\mu_\alpha}. \tag{5}$$

Substituting Equations (2) and (3) into Equation (1), the mass conservation equations for the α-phase reads:

$$\partial_t S_\alpha + \partial_x v_\alpha = 0, \qquad \alpha = w, o, g. \tag{6}$$

Equations (6) are not all independent from each other, because they have to satisfy the constraint that the fluids fill up the pore space, $S_w + S_o +$

$S_g \equiv 1$. The *fractional flow approach* decouples the problem into a "pressure equation" and a system of "saturation equations" [15]. Summation of the conservation equations for all phases and use of the saturation constraint yields the pressure equation:

$$\partial_x v_T = 0, \tag{7}$$

where $v_T := v_w + v_o + v_g$ is the total velocity. The pressure equation dictates that the total velocity v_T is at most a function of time. Using the expression of the fluid velocities in Equation (4), we express the total velocity as:

$$v_T = -\frac{k}{\phi}(\lambda_T \partial_x p + (\rho_w \lambda_w + \rho_o \lambda_o + \rho_g \lambda_g) g_x), \tag{8}$$

where $\lambda_T := \lambda_w + \lambda_o + \lambda_g$ is the total mobility. With the definitions above, the system of saturation equations governing three-phase flow is:

$$\begin{aligned} \partial_t S_w + v_T \partial_x \left[\frac{\lambda_w}{\lambda_T} \left(1 - \frac{k}{v_T \phi} g_x \big((\rho_w - \rho_o)\lambda_o + (\rho_w - \rho_g)\lambda_g \big) \right) \right] = 0, \\ \partial_t S_g + v_T \partial_x \left[\frac{\lambda_g}{\lambda_T} \left(1 + \frac{k}{v_T \phi} g_x \big((\rho_w - \rho_g)\lambda_w + (\rho_o - \rho_g)\lambda_o \big) \right) \right] = 0, \end{aligned} \tag{9}$$

together with the saturation constraint $S_o = 1 - S_w - S_g$. In what follows we shall assume that the total velocity v_T is constant, and not a generic function of time.

2.2 Equations in dimensionless form

It is convenient to express the system (9) in dimensionless form. To this end, we define the following variables:

$$x_D := \frac{x}{L} \qquad \text{(dimensionless space)}, \tag{10}$$

$$t_D := \frac{v_T\, t}{L} \qquad \text{(dimensionless time)}, \tag{11}$$

$$N_D := \frac{(\rho_o - \rho_g)k}{\mu_o v_T \phi}\, g_x \qquad \text{(gravity number)}, \tag{12}$$

$$\rho_D := \frac{\rho_w - \rho_g}{\rho_o - \rho_g} \qquad \text{(density ratio)}. \tag{13}$$

With definitions (10)–(13), the 2×2 system of saturation equations (9) takes the standard form

$$\frac{\partial}{\partial t_D} \begin{pmatrix} S_w \\ S_g \end{pmatrix} + \frac{\partial}{\partial x_D} \begin{pmatrix} f_w \\ f_g \end{pmatrix} = \begin{pmatrix} 0 \\ 0 \end{pmatrix}, \tag{14}$$

where the water and gas flux functions have the following expressions:

$$\begin{aligned} f_w &:= \frac{\lambda_w}{\lambda_T} \left[1 - N_D \left((\rho_D - 1) k_{ro} + \rho_D \frac{\mu_o}{\mu_g} k_{rg} \right) \right], \\ f_g &:= \frac{\lambda_g}{\lambda_T} \left[1 + N_D \left(\rho_D \frac{\mu_o}{\mu_w} k_{rw} + k_{ro} \right) \right], \end{aligned} \tag{15}$$

or, alternatively,

$$\begin{aligned} f_w &:= \frac{\lambda_w}{\lambda_T} \left[1 - M \left((\rho_D - 1) \lambda_o + \rho_D \lambda_g \right) \right], \\ f_g &:= \frac{\lambda_g}{\lambda_T} \left[1 + M \left(\rho_D \lambda_w + \lambda_o \right) \right], \end{aligned} \tag{16}$$

where $M := N_D \mu_o$. Defining the equivalent vector notation:

$$\boldsymbol{u} := \begin{pmatrix} u \\ v \end{pmatrix} \equiv \begin{pmatrix} S_w \\ S_g \end{pmatrix}, \qquad \boldsymbol{f} := \begin{pmatrix} f \\ g \end{pmatrix} \equiv \begin{pmatrix} f_w \\ f_g \end{pmatrix}, \tag{17}$$

and understanding the space and time variables as their dimensionless counterparts —equations (10)–(11), the system (14) can be written in its final form:

$$\partial_t \boldsymbol{u} + \partial_x \boldsymbol{f} = \boldsymbol{0}. \tag{18}$$

After a change of variables, the vector of unknowns $\boldsymbol{u}$ can be understood as the vector of *reduced* saturations, rather than *actual* saturations [35]. When this renormalization is employed, the three-phase flow region —where all three phases are mobile— covers the entire saturation triangle.

2.3 Character of the system of equations

The classification of the system (18) reduces to analyzing the behavior of the eigenvalue problem

$$\boldsymbol{A}\boldsymbol{r} = \nu \boldsymbol{r}, \tag{19}$$

where

$$\boldsymbol{A} := \boldsymbol{f}' \equiv \mathrm{D}_{\boldsymbol{u}}\boldsymbol{f} \equiv \begin{pmatrix} f_{,u} & f_{,v} \\ g_{,u} & g_{,v} \end{pmatrix} \tag{20}$$

is the Jacobian matrix of the system, ν is an eigenvalue, and $\boldsymbol{r}$ is a right eigenvector. Subscripts after a comma denote differentiation (*e.g.*, $f_{,u} \equiv \partial_u f$). At any saturation state $\boldsymbol{u}$, the system may be of one of the following types [35]:

1. *Strictly hyperbolic.* The eigenvalue problem has two real, distinct eigenvalues. The Jacobian matrix is diagonalizable and there are two real and linearly independent eigenvectors.

2. *Elliptic.* The eigenvalues are complex conjugates, and there are no real characteristic curves.

3. *Nonstrictly hyperbolic.* There is a double real eigenvalue, and the Jacobian matrix is diagonalizable. Every direction is characteristic, so the system is hyperbolic (real eigenvalues and linearly independent eigenvectors) but not strictly hyperbolic (which requires that the eigenvalues be distinct).

4. *Parabolic.* The system has a real, double eigenvalue, and the Jacobian matrix is defective (non-diagonalizable). There is only one eigenvector and, therefore, there is only one real characteristic direction.

The *eigenvalues* $\nu_i,\ i = 1, 2$ of the Jacobian matrix (20) are given by:

$$\nu_{1,2} = \frac{1}{2}\left[f_{,u} + g_{,v} \mp \sqrt{(f_{,u} - g_{,v})^2 + 4 f_{,v} g_{,u}} \right]. \tag{21}$$

These eigenvalues (when they are real) are the characteristic speeds at which waves describing changes in saturation propagate through the domain. In the strictly hyperbolic case, there exist two distinct waves which travel at different characteristic speeds. It is common to use the terms *slow wave* and *fast wave* for the waves associated with the smaller and larger eigenvalue, respectively.

The *right eigenvectors* $\boldsymbol{r}_i = [r_{iu}, r_{iv}]^t,\ i = 1, 2$, which correspond to eigenvalues $\nu_i,\ i = 1, 2$, respectively, are calculated by the following expressions:

$$\frac{r_{1v}}{r_{1u}} = \frac{\nu_1 - f_{,u}}{f_{,v}} = \frac{g_{,u}}{\nu_1 - g_{,v}}, \tag{22}$$

$$\frac{r_{2u}}{r_{2v}} = \frac{f_{,v}}{\nu_2 - f_{,u}} = \frac{\nu_2 - g_{,v}}{g_{,u}}. \tag{23}$$

When they are real, the right eigenvectors correspond to the directions (in the saturation space) of admissible changes in saturation. In the strictly hyperbolic case, the changes in saturation associated with the slow (resp. fast) wave have a direction dictated by $\boldsymbol{r}_1$ (resp. $\boldsymbol{r}_2$) and propagate with velocity ν_1 (resp. ν_2).

3 Conditions for a strictly hyperbolic system

It is by now a well-known fact that the system of equations (18) describing one-dimensional three-phase flow may exhibit mixed hyperbolic/elliptic character for most relative permeability functions used today [13, 17, 18, 21, 24, 25, 32, 34, 44, 52, 53]. Strict hyperbolicity of the equations is typically lost at:

1. *Elliptic regions:* bounded regions of the saturation triangle, where the eigenvalues are complex conjugates, and the system is locally elliptic.

2. *Umbilic points:* saturation states for which there is a double eigenvalue, and the system is *not* strictly hyperbolic.

The existing literature seems to suggest that the presence of elliptic regions and umbilic points *inside* the saturation triangle is an unavoidable feature of three-phase flow models in porous media. The approach taken in previous investigations [32,52] is to *assume* a particular behavior of the relative permeabilities and, from this assumed behavior, infer that the system of equations cannot be strictly hyperbolic everywhere in the saturation triangle. One of the key assumptions is the "zero-derivative" condition, which states that the relative permeability of a phase has a zero normal derivative at the edge of zero saturation of that phase. This condition implies, for example, that the derivative of the gas relative mobility with respect to gas saturation is zero

along the oil-water edge of the saturation triangle:

$$\lambda_{g,v} = 0 \quad \text{on } v = 0,\ 0 < u < 1. \tag{24}$$

Under this assumed behavior along the edges of the saturation triangle, it can be shown that an elliptic region must be present inside the ternary diagram [32, 51, 52].

When gravity is included in the formulation, it was shown that a large class of models of three-phase relative permeabilities may yield elliptic regions [57] (see also [24, 25, 33, 34, 53]). Common to all these investigations is the use of Muskat's multiphase flow extension of Darcy's equation, and relative permeabilities which are taken as fixed functions of saturations independent of the flow regime. Under these assumptions, the analysis in [57] shows that for any relative permeability model where one or more relative permeabilities are functions of two saturations, the system of saturation equations will have elliptic regions for some combination of viscosities, densities and gravity numbers.

We find the mixed elliptic/hyperbolic behavior disturbing for many reasons, and are of the opinion that elliptic regions are artifacts of an incorrect mathematical model. In a previous paper [35], we have argued that strict hyperbolicity is an essential property of a displacement process, which should be preserved by our three-phase flow models. From an analysis of the character of the system of equations governing three-phase immiscible incompressible flow we conclude that —when gravity effects are not included— it is possible to choose relative permeability functions so that this system is strictly hyperbolic everywhere in the saturation triangle. Moreover, the generic conditions that need to be imposed on the relative permeability functions to preserve strict hyperbolicity seem to be in agreement with experimental observations and pore-scale physics.

The question remains: is it possible to derive similar conditions when gravity is included, so that the system of saturation equations is strictly hyperbolic? The analysis of Trangenstein [57] suggests that the answer is negative. His analysis is limited, however, by the fact that *fixed* relative permeability functions are used. Ellipticity of the equations arises because the "driving force" in Equation (4) is modified by including a dominant gravity term, while the relative permeability functions are kept unchanged. In our opinion, using fixed relative permeability functions for all gravity numbers is not realistic. Dominance of gravity forces modifies the displacements of

one fluid by another which, in turn, may yield different macroscopic relative permeabilities. Thus, in the analysis below, we adopt the opposite viewpoint to that of previous investigations: we do *not* rule out the possibility that the macroscopic relative permeabilities may depend on the gravity number. In doing so, we acknowledge that the common extension of Darcy's equation does not capture all the physics of multiphase flow.

3.1 Conceptual picture of three-phase displacements

The behavior of relative permeabilities, assumed in traditional models of three-phase flow, limits the influence of a phase on the flow of the other two phases near the edge where that phase is immobile [32, 52]. This behavior is expressed effectively through the eigenvectors of the Jacobian matrix of the system of governing equations along the edges of the ternary diagram (Figure 1):

1. The right eigenvector associated with the fast characteristic family, $\boldsymbol{r}_2$, is *parallel* to the edges of the triangle of reduced saturations.

2. The fast eigenvector $\boldsymbol{r}_2$ points *into* the triangle, for saturation states near the vertices.

The most relevant impact of this conceptual picture on the mathematical character of the system is that, in general, an elliptic region must exist inside the saturation triangle. This general result can be proved using ideas of projective geometry [32, 51, 52].

Our conceptual picture of three-phase displacements differs from the traditional one. The difference, although subtle, is essential. The key observation is that, whenever gas is present as a continuous phase, the mobility of gas is much higher than that of the other two fluids (water and oil). This implies that the wave associated with changes in gas saturation is in fact the fast wave, even in the neighborhood of the edge of zero reduced gas saturation. The proposed behavior requires that the eigenvector of the fast characteristic family ($\boldsymbol{r}_2$) is *transversal* —and not parallel— to the oil-water edge of the ternary diagram (Figure 2). In [35] we showed that this conceptual picture permits that the system of equations be strictly hyperbolic everywhere *inside* the saturation triangle. The only saturation state for which strict hyperbolicity is lost is the vertex of 100% reduced gas saturation, due to the additional

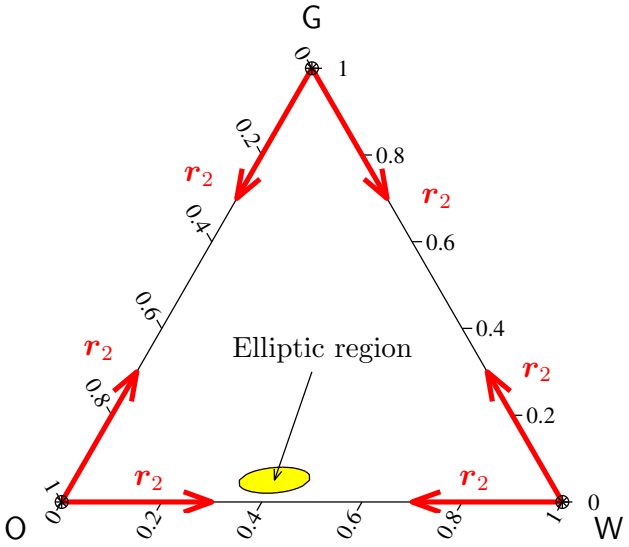

Figure 1. Schematic representation of the direction of fast eigenvectors $\boldsymbol{r}_2$ along the edges of the saturation triangle for the models analyzed by Shearer [52] and Holden [32]. For models of this type, vertices are umbilic points, and there must be an elliptic region inside the saturation triangle.

requirement that the eigenvectors are not allowed to rotate along the edges of the ternary diagram.

The picture of slow and fast characteristic paths along the edges of the saturation triangle shown in Figure 2 was developed for the case where gravity effects were not included in the formulation [35]. We preserve this conceptual picture when gravity effects are taken into account. This is sensible, however, only if the three-phase flow is a *displacement process*. Therefore, we limit our description of three-phase flow with gravity to situations of *co-current* flow, that is, when all three phases have fluid velocities that contribute positively to the total flow. In fact, the situation changes dramatically if flow of one of the fluids is counter-current for certain saturation states. It is obvious that flow *cannot* be counter-current in the entire saturation triangle and, therefore, mixed co-current and counter-current flow will take place for certain saturation paths. In this case, capillarity effects cannot be neglected and the three-phase displacement model analyzed here is no longer valid.

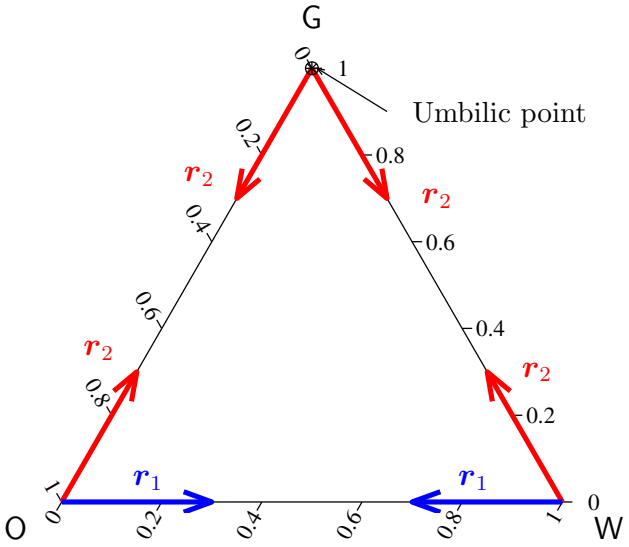

Figure 2. Schematic representation of the direction of fast ($\boldsymbol{r}_2$) and slow ($\boldsymbol{r}_1$) eigenvectors along the edges of the saturation triangle for the type of models we propose. The system is strictly hyperbolic everywhere inside the saturation triangle, and the only umbilic point is located at the G vertex, where the fast paths corresponding to the OG and WG edges coalesce.

In summary, we restrict our attention to displacement processes, characterized by co-current flow. In the following sections we derive mathematical conditions for co-current flow and strict hyperbolicity of the system.

3.2 Conditions for co-current flow

The conditions for co-current flow can be expressed succinctly as follows:

$$f \geq 0, \tag{25}$$

$$g \geq 0, \tag{26}$$

$$1 - f - g \geq 0. \tag{27}$$

When written in terms of the relative mobilities (Equations (16)), the equations above take the following form:

$$1 - M(\rho_D \lambda_g + (\rho_D - 1)\lambda_o) > 0, \tag{25'}$$

$$1 + M(\rho_D \lambda_w + \lambda_o) > 0, \tag{26'}$$

$$1 - M(\lambda_g - (\rho_D - 1)\lambda_w) > 0. \tag{27'}$$

Conditions (25′)–(27′) must hold for any saturation state in the ternary diagram. It is possible, however, to ascertain which saturation states impose the most restrictive constraints on the gravity number.

Condition (25′) of positive *water* fractional flow will impose the strictest restriction on the gravity number wherever the factor $\Xi_w := (\rho_D - 1)\lambda_o + \rho_D \lambda_g$ is largest. The oil and gas relative mobilities will increase as the water saturation decreases. Therefore, it will be sufficient to analyze the factor Ξ_w on the OG edge, where the reduced water saturation is zero. Moreover, the functions λ_o and λ_g are *convex* along the OG edge, so Ξ_w will take a maximum value at one of the vertices, corresponding to either 100% reduced oil saturation (the O vertex) or 100% reduced gas saturation (the G vertex). In all practical cases, the gas viscosity is much smaller than the oil viscosity ($\mu_g \ll \mu_o$) and, as a result, Ξ_w will be largest at the G vertex. Evaluating condition (25′) at this saturation state, one obtains:

$$M < \frac{1}{\rho_D \lambda_g^{\max}}, \tag{28}$$

or, equivalently,

$$N_D < \frac{\mu_g}{\mu_o} \frac{1}{\rho_D k_{rg}^{\max}}. \tag{29}$$

Condition (27′) of positive *oil* fractional flow can be analyzed similarly. In this case, the strictest restriction on the gravity number occurs at the saturation state for which the factor $\Xi_o := -(\rho_D - 1)\lambda_w + \lambda_g$ is largest. Following the same arguments as above, this happens at the G vertex, where Condition (27′) reduces to

$$M < \frac{1}{\lambda_g^{\max}}, \tag{30}$$

or, equivalently,

$$N_D < \frac{\mu_g}{\mu_o} \frac{1}{k_{rg}^{\max}}. \tag{31}$$

The condition of positive *gas* fractional flow requires that the inequality (26′) be satisfied. The strictest condition arises when the factor $\Xi_g := \rho_D \lambda_w + \lambda_o$ reaches maximum. This will happen at one of the two vertices on the OW edge of zero reduced gas saturation. Evaluating this condition at both vertices, one obtains the following restriction:

$$M > \max\left\{\frac{-1}{\rho_D \lambda_w^{\max}}; \frac{-1}{\lambda_o^{\max}}\right\} \tag{32}$$

or, equivalently,

$$N_D > \max\left\{-\frac{\mu_w}{\mu_o}\frac{1}{\rho_D k_{rw}^{\max}}; \frac{-1}{k_{ro}^{\max}}\right\}. \tag{33}$$

Conditions (29), (31) and (33) for co-current flow can be summarized succinctly in the following restriction on M:

$$\max\left\{\frac{-1}{\rho_D \lambda_w^{\max}}; \frac{-1}{\lambda_o^{\max}}\right\} < M < \min\left\{\frac{1}{\rho_D \lambda_g^{\max}}; \frac{1}{\lambda_g^{\max}}\right\} \tag{34}$$

or, equivalently, on the gravity number N_D:

$$\max\left\{-\frac{\mu_w}{\mu_o}\frac{1}{\rho_D k_{rw}^{\max}}; \frac{-1}{k_{ro}^{\max}}\right\} < N_D < \min\left\{\frac{\mu_g}{\mu_o}\frac{1}{\rho_D k_{rg}^{\max}}; \frac{\mu_g}{\mu_o}\frac{1}{k_{rg}^{\max}}\right\}. \tag{35}$$

We restrict our analysis to the case when this condition is satisfied.

3.3 Conditions for strict hyperbolicity

The derivation of necessary conditions for strict hyperbolicity of the system of governing equations is based on the conceptual picture expressed in Figure 2:

1. Along the oil-water (OW) edge, the eigenvector associated with the *slow* characteristic family ($\boldsymbol{r}_1$) is parallel to the edge. The system is strictly hyperbolic everywhere along the edge, including the O and W vertices.

2. Along the oil-gas (OG) and water-gas (WG) edges, the eigenvector associated with the *fast* characteristic family ($\boldsymbol{r}_2$) is parallel to these edges. The system is strictly hyperbolic everywhere along the edges except at the G vertex, which is an umbilic point.

Along each of the three edges, two types of conditions need to be imposed:

Table 1. Summary of conditions for strict hyperbolicity along the edges of the saturation triangle, in terms of the fractional flow functions.

	OW edge	OG edge	WG edge
Condition I	$g_{,u} = 0$	$f_{,v} = 0$	$f_{,v} + g_{,v} = f_{,u} + g_{,u}$
Condition II	$g_{,v} - f_{,u} > 0$	$g_{,v} - f_{,u} > 0$	$-g_{,u} - f_{,v} > 0$

Condition I enforces that eigenvectors of the appropriate family are parallel to the edge.

Condition II enforces strict hyperbolicity along the edge.

We shall not repeat the entire analysis along each of the edges of the saturation triangle, and we refer the reader to [35] for the mathematical considerations that lead to the conditions shown in Table 1. When these conditions are expressed in terms of fluid relative mobilities through Equations (16), we obtain restrictions that the relative mobilities must satisfy for the system to be strictly hyperbolic. The conditions along the *edges* are summarized in Table 2, and the conditions at the *vertices* of the saturation triangle are given in Table 3. The analysis is analogous to that carried out for the case without gravity, the only difference being that the water and gas fractional flows (f and g, respectively) have more complicated expressions due to the gravity term.

3.4 Discussion of conditions

Several aspects of the conditions for strict hyperbolicity derived above deserve further discussion and interpretation.

1. If the gravity number is zero, the conditions reduce to those obtained in [35], where gravity was not included in the analysis.

2. It is interesting to see how the conditions for co-current flow relate to the conditions for strict hyperbolicity. When specialized to each of the three edges (that is, $\lambda_g = 0$ along the OW edge, $\lambda_w = 0$ along the OG edge, and $\lambda_o = 0$ along the WG edge), relations (25′)–(27′) imply that all the terms in square brackets in Table 2 are strictly positive. Similarly, if the co-current flow conditions are specialized at the vertices

Table 2. Summary of conditions for strict hyperbolicity along the edges of the saturation triangle, in terms of the fluid relative mobilities.

Condition I	
OW edge:	$\lambda_{g,u} = 0$
OG edge:	$\lambda_{w,v} = 0$
WG edge:	$\lambda_{o,v} = \lambda_{o,u}$
Condition II	
OW edge:	$(\lambda_w + \lambda_o)[1 + M(\rho_D \lambda_w + \lambda_o)]\lambda_{g,v}$ $> \lambda_o[1 - M(\rho_D - 1)\lambda_o]\lambda_{w,u} - \lambda_w[1 + M(\rho_D - 1)\lambda_w]\lambda_{o,u}$
OG edge:	$(\lambda_g + \lambda_o)[1 - M(\rho_D \lambda_g + (\rho_D - 1)\lambda_o)]\lambda_{w,u}$ $< \lambda_o[1 + M\lambda_o]\lambda_{g,v} - \lambda_g[1 - M\lambda_g]\lambda_{o,v}$
WG edge:	$(\lambda_g + \lambda_w)[1 - M(\lambda_g - (\rho_D - 1)\lambda_w)](-\lambda_{o,u})$ $< \lambda_w[1 + M\rho_D\lambda_w](\lambda_{g,v} - \lambda_{g,u}) + \lambda_g[1 - M\rho_D\lambda_g](\lambda_{w,u} - \lambda_{w,v})$

Table 3. Summary of conditions for strict hyperbolicity at the vertices of the saturation triangle, in terms of the fluid relative mobilities.

Condition I	
O vertex:	$\lambda_{g,u} = 0; \quad \lambda_{w,v} = 0$
W vertex:	$\lambda_{g,u} = 0; \quad \lambda_{o,v} = \lambda_{o,u}$
G vertex:	$\lambda_{w,v} = 0; \quad \lambda_{o,v} = \lambda_{o,u}$
Condition II	
O vertex:	$\lambda_{g,v} > \dfrac{1 - M(\rho_D - 1)\lambda_o}{1 + M\lambda_o}\lambda_{w,u}$
W vertex:	$\lambda_{g,v} > \dfrac{1 + M(\rho_D - 1)\lambda_w}{1 + M\rho_D\lambda_w}(-\lambda_{o,u})$
G vertex:	$\lambda_{w,u} = \dfrac{1 - M\lambda_g}{1 - M\rho_D\lambda_g}(-\lambda_{o,u})$

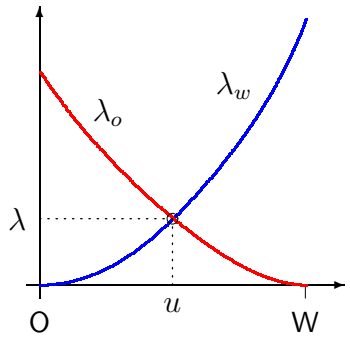

Figure 3. Schematic of the profiles of water and oil relative mobilities along the OW edge. The value u corresponds to the reduced water saturation for which oil and water relative mobilities are equal: $\lambda_w = \lambda_o = \lambda$.

of the saturation triangle, it is immediate to see that both the numerator and denominator of the fractions in Table 3 are strictly positive also. These restrictions, which arise *physically* from limiting our study to co-current flow, are crucial to obtaining a strictly hyperbolic model. Indeed, only in co-current flow it is possible to satisfy the conditions for strict hyperbolicity with *finite* derivatives of the relative mobilities.

3. A positive derivative of the gas relative mobility with respect to gas saturation along the OW edge is the fundamental requirement for strict hyperbolicity of the system. It means that the gas relative permeability curve —as a function of its own saturation— must have a positive slope at its endpoint saturation. This essential condition was first identified in [35], where it was justified in terms of pore-scale fluid displacements, and shown to be in good qualitative agreement with experimental data.

4. The condition of a positive endpoint-slope of the gas relative permeability is generalized in this paper to account for gravity effects. To better understand the influence of gravity, we study this condition at a saturation state $(u, 0)$ on the OW edge such that the water and the oil relative mobilities are equal (see Figure 3), that is,

$$\lambda_w(u, 0) = \lambda_o(u, 0) = \lambda. \tag{36}$$

The condition for strict hyperbolicity at this saturation state reduces

to:

$$\lambda_{g,v} > \lambda_{g,v}^{\min} = \frac{1}{2}[\lambda_{w,u} - \lambda_{o,u}] - \frac{M\lambda}{1 + M(\rho_D + 1)\lambda}[\rho_D \lambda_{w,u} - \lambda_{o,u}]. \quad (37)$$

Since $\rho_D > 0$, it is evident that the terms enclosed in brackets in expression (37) are always positive. Because the density and viscosity of gas are much lower than those of water and oil, it is reasonable to think that gravity will influence the relative mobility of gas more than the relative mobilities of oil and water. Thus, we may assume that $\lambda_{w,u}$ and $\lambda_{o,u}$ do not vary greatly with the gravity number. Under this assumption, we find that the *minimum* endpoint-slope of the gas relative mobility, $\lambda_{g,v}^{\min}$, shows the following trend with the gravity number:

$$\lambda_{g,v}^{\min}\big|_{M<0} \geq \lambda_{g,v}^{\min}\big|_{M=0} \geq \lambda_{g,v}^{\min}\big|_{M>0}\,. \quad (38)$$

5. The dependence of the minimum endpoint-slope of the gas relative permeability on the gravity number can be interpreted and justified from the point of view of the displacement processes taking place in the porous medium. We may have two different cases:

   (a) *Increasing gas saturation.* This is a drainage process, because gas is normally the least wetting phase. For visualization, it is helpful to understand it as a gas injection. The slope of the gas relative permeability curve will be related to the behavior of the *first percolating cluster*. If flow is in the direction opposite to gravity ($M > 0$), the gas displacement will tend to be less stable than in the case of horizontal flow [38, 59]. At any given cross-section of the porous medium, the transition between zero gas flow and nonzero gas flow will be less abrupt. This gentler transition will translate into a smaller endpoint-slope of the gas relative permeability. On the other hand, if flow is in the direction of the gravity force ($M < 0$), the displacement will be stabler than for horizontal flow. In this case, an abrupt transition from zero to nonzero gas flow is expected, resulting in a larger endpoint-slope of the gas relative permeability function.

   (b) *Decreasing gas saturation.* We associate this type of displacement with imbibition, where fluids of higher wettability than gas — water and oil— are injected into the porous medium. There is an

essential difference with respect to a drainage process: because gas is the least wetting fluid, there are now mechanisms for trapping of the gas phase. Therefore, the behavior of the relative permeability curve in the neighborhood of zero mobile gas saturation will be determined by the *last trapped cluster*. In the case of flow upwards ($M > 0$), gravity effects will enhance the stability of gas displacement by water and oil [38, 60], resulting in a smaller fraction of "disconnected" gas clusters and a more gradual sweeping of the gas phase. This continuous dependence of the gas flow on the amount of gas present will translate into a smaller endpoint-slope of the gas relative permeability. In contrast, when flow is in the direction of gravity ($M < 0$), the displacement process is less stable. It is more likely that water and oil will take the most favorable paths, leaving behind large amounts of gas. These paths may eventually merge and form disconnected —trapped— gas clusters. At any given cross-section of the flow domain, the transition between nonzero and zero gas flow may occur for very small changes in gas saturation. It seems natural to reproduce this behavior through a larger endpoint-slope of the gas relative permeability.

6. It would be interesting to validate, at least qualitatively, the conditions obtained in this paper with experiments. However, this was not pursued here.

4 A simple model

The purpose of this section is to demonstrate it is indeed possible to devise relative permeability models that satisfy the conditions for co-current flow and strict hyperbolicity derived in Section 3. As a result, the system of equations describing three-phase co-current flow with gravity will be strictly hyperbolic everywhere inside the saturation triangle. To illustrate our analysis, we use the following model of relative mobilities:

$$\lambda_w = (1/\mu_w)u^2, \tag{39}$$

$$\lambda_g = (1/\mu_g)\left(\beta_g v + (1-\beta_g)v^2\right), \tag{40}$$

$$\lambda_o = (1/\mu_o)(1-u-v)(1-u)(1-v). \tag{41}$$

This model belongs to a widely used class of models [55, 56], where the water and gas relative permeabilities depend solely on their own saturations, whereas the oil relative permeability depends on two saturations. The most important features of this model are:

1. The only relative permeability function whose form is allowed to change with the viscosity ratio and the gravity number is the *gas* relative permeability. This is accomplished here in the simplest possible way, through a single parameter: the endpoint-slope β_g.

2. In view of the conditions for co-current flow and strict hyperbolicity derived in the previous section, we anticipate that the endpoint-slope of the gas relative permeability function will be positive, that is, $\beta_g > 0$.

4.1 Conditions for co-current flow

It is immediate to specialize condition (35) on the allowable range of the gravity number N_D to the simple model studied here. Because the relative permeability functions are assumed to be normalized, we take $k_{r\alpha}^{\max} = 1$, $\alpha = w, o, g$. Defining the viscosity ratios:

$$\mu_D^w := \mu_w / \mu_o, \tag{42}$$

$$\mu_D^g := \mu_g / \mu_o, \tag{43}$$

we express the conditions for co-current flow as follows:

$$\max\left\{-\frac{\mu_D^w}{\rho_D}; -1\right\} < N_D < \min\left\{\frac{\mu_D^g}{\rho_D}; \mu_D^g\right\}. \tag{44}$$

4.2 Conditions for strict hyperbolicity

It can be readily checked that the relative permeability model (39)–(41) automatically satisfies *Condition I* (see Tables 1 and 2), which imposes that eigenvectors do not rotate along the edges of the saturation triangle.

Condition II for strict hyperbolicity along the edges of the ternary diagram (Table 1) reads:

$$H_{ow} := g_{,v} - f_{,u} > 0 \qquad \text{along the OW edge,} \tag{45}$$

$$H_{og} := g_{,v} - f_{,u} > 0 \qquad \text{along the OG edge,} \tag{46}$$

$$H_{wg} := -g_{,u} - f_{,v} > 0 \qquad \text{along the WG edge.} \tag{47}$$

When gravity is not included in the analysis, it is possible to obtain closed-form expressions on the parameter β_g, so that these conditions are satisfied [35]. This is not viable in the present case, because gravity effects yield much more complicated expressions.

4.2.1 Analysis along the OW edge.

Specializing the relative permeabilities to the OW edge (that is, $v = 0,\ 0 \leq u \leq 1$), substituting the expressions into condition (45) (see also Table 2), and after some algebraic manipulations, we obtain:

$$\begin{aligned} H_{ow} \propto & \left(u^2/\sqrt{\mu_D^w} + \sqrt{\mu_D^w}(1-u)^2\right)\left[1 + N_D(\frac{\rho_D}{\mu_D^w}u^2 + (1-u)^2)\right]\frac{\sqrt{\mu_D^w}}{\mu_D^g}\beta_g \\ & - 2\left[1 - N_D(\rho_D - 1)(1-u)^2\right](1-u)^2 u \\ & - 2\left[1 + N_D\frac{\rho_D - 1}{\mu_D^w}u^2\right]u^2(1-u) > 0. \end{aligned} \tag{48}$$

The expression above translates into a condition on the endpoint-slope β_g of the gas relative permeability as a function of the dimensionless parameters:

$$\beta_g > \beta_g^{\min} := \frac{\mu_D^g}{\sqrt{\mu_D^w}} \max_{0 \leq u \leq 1} \left\{F(u; N_D, \mu_D^w, \rho_D)\right\}, \tag{49}$$

where

$$F := 2\frac{\left[1 - N_D(\rho_D - 1)(1-u)^2\right](1-u)^2 u + \left[1 + N_D\frac{\rho_D - 1}{\mu_D^w}u^2\right]u^2(1-u)}{\left(u^2/\sqrt{\mu_D^w} + \sqrt{\mu_D^w}(1-u)^2\right)\left[1 + N_D(\frac{\rho_D}{\mu_D^w}u^2 + (1-u)^2)\right]}. \tag{50}$$

It is worth noting that the restrictions on the gravity number due to the co-current flow conditions imply that all terms in square brackets in Equation (50) are positive.

4.2.2 Analysis along the OG edge.

Specializing the relative mobilities at the OG edge ($u = 0,\ 0 < v < 1$), condition (46) reads:

$$\begin{aligned} H_{og} \propto & \ 2\left(1 - \frac{N_D}{\mu_D^g}v^2\right)(1-v) - 2\left[1 + N_D(1-v)^2\right](1-v)^2 v \\ & - \left(2\frac{N_D}{\mu_D^g}v(1-v)^2 + \left[1 + N_D(1-v)^2\right](1-v)^2(1-2v)\right)\beta_g > 0. \end{aligned} \tag{51}$$

Although difficult to derive analytically, it can be checked that condition (51) is always satisfied as long as the conditions of co-current flow are met. The analytical calculations may be carried out in the neighborhood of the G vertex. If we let $v = 1 - \varepsilon$, the first-order Taylor expansion of H_{og} about $\varepsilon = 0$ is:

$$H_{og} \propto 2\varepsilon + O(\varepsilon^2) > 0. \tag{52}$$

At $\varepsilon = 0$, $H_{og} = 0$, so that the G vertex is an umbilic point, as required. For all states on the OG edge near the G vertex, $H_{og} > 0$, and the system is strictly hyperbolic.

4.2.3 Analysis along the WG edge.

We study the strict hyperbolicity condition along the WG edge following the same procedure. As was the case for the analysis on the OG edge, the condition $H_{wg} > 0$ is difficult to verify analytically. It was found, however, that if it is satisfied in the neighborhood of the G vertex, it is also satisfied everywhere along the edge. Therefore, we analyze this condition for a saturation state $(u, v) = (\varepsilon, 1 - \varepsilon)$. The first-order Taylor expansion about $\varepsilon = 0$ reads:

$$H_{wg} \propto \big((2 - \mu_D^w) - (2\rho_D - \mu_D^w)N_D/\mu_D^g\big)\varepsilon + O(\varepsilon^2) > 0. \tag{53}$$

For condition (53) to be satisfied, we require that:

$$\mu_D^w < \min\{2\rho_D; 2\}, \tag{54}$$

$$N_D < \mu_D^g \frac{2 - \mu_D^w}{2\rho_D - \mu_D^w}. \tag{55}$$

Condition (54) is a generalization of its counterpart in [35] when gravity was not included. In general, inequality (55) may or may not be satisfied automatically by the co-current flow conditions (44). Conditions (54)–(55) should be understood as limits of applicability of the *relative permeability model*, rather than physical restrictions on the actual values that the viscosity ratio and the gravity number may take.

4.2.4 An example

We present a particular example where, after fixing all the dimensionless parameters, we examine the admissible range of values for the endpoint-slope β_g

of the gas relative permeability, so that the system is strictly hyperbolic. In particular, we take:

$$\rho_D = 1.2; \quad \mu_D^w = 0.5; \quad \mu_D^g = 0.04. \tag{56}$$

To satisfy the co-current flow condition (44), the gravity number must be within the interval

$$-5/12 < N_D < 3/90. \tag{57}$$

Substituting the density and viscosity ratios in (56) into condition (55), the gravity number is also restricted by:

$$N_D < 3/95, \tag{58}$$

which is less than the upper bound in (57). Therefore, the gravity number is allowed to vary between $-5/12 < N_D < 3/95$.

In Figure 4 we show the region of admissible values of β_g such that condition (49) along the OW edge is satisfied. This condition turns out to be the essential requirement for strict hyperbolicity of the system. It will be met whenever β_g is greater than a positive *minimum* endpoint-slope $\beta_g^{\min}$, which depends on the gravity number N_D. The value $\beta_g^{\min}$ decreases with increasing gravity number. This dependence is consistent with the physical behavior described in Section 3.4 (see expression (38)). It is important to note that $\beta_g^{\min}$ is a *lower bound* for the endpoint-slope of the gas relative permeability, and *not* the required value. Therefore, the actual slope may display a wider variation with the gravity number than that of $\beta_g^{\min}$.

To illustrate the effect of the endpoint-slope β_g of the gas relative permeability on the character of the system of equation, we take a fixed value of the gravity number,

$$N_D = -0.4, \tag{59}$$

and analyze two different values of β_g, one violating condition (49), and the other one satisfying it:

$$\beta_g^{\text{ell}} = 0, \quad \beta_g^{\text{hyp}} = 0.1. \tag{60}$$

The relative permeability of gas as a function of its own reduced saturation, given by Equation (40), is shown in Figure 5 for the two values of the endpoint-slope β_g above. It is noteworthy that both curves are very close to one another and, would, in principle, match relative permeability data equally well (or equally badly). However, the implications of using one

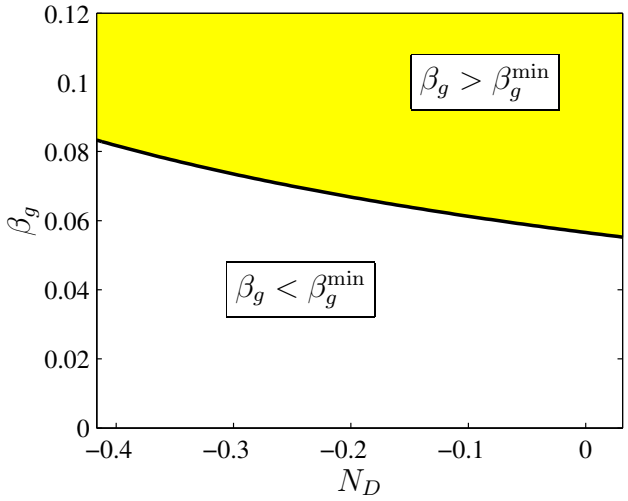

Figure 4. Admissible values of the endpoint-slope β_g of the gas relative permeability as a function of the gravity number N_D, for the gravity and viscosity ratios in Equation (56). The shaded area ($\beta_g > \beta_g^{\min}$) represents the set of values of the parameter β_g for which the system is strictly hyperbolic everywhere in the saturation triangle.

endpoint-slope or the other are far-reaching: one will yield a system of equations with mixed elliptic/hyperbolic behavior, while the other will produce a system that is everywhere strictly hyperbolic.

In Figure 6 we plot the functions $H_{ow}(u)$ along OW, $H_{og}(v)$ along OG, and $H_{wg}(u)$ along WG, for each of the two values of β_g. The curves along the OG edge and the WG edge reach a zero value for $v = 1$ and $u = 0$, respectively, so that the G vertex is an umbilic point. Inequalities (45)–(47) are satisfied —and the system is strictly hyperbolic— if all three curves are positive everywhere. As expected, this condition is violated when the value $\beta_g = 0$ is used —Figure 6(a)— and it is satisfied when $\beta_g = 0.1$ is employed —Figure 6(b).

For each of these two cases we search for elliptic regions in the saturation triangle. An elliptic region is a set of points in the saturation space where the eigenvalues of the Jacobian matrix of the system of governing equations are complex conjugates. Thus, the (complex) eigenvalues at any point in the

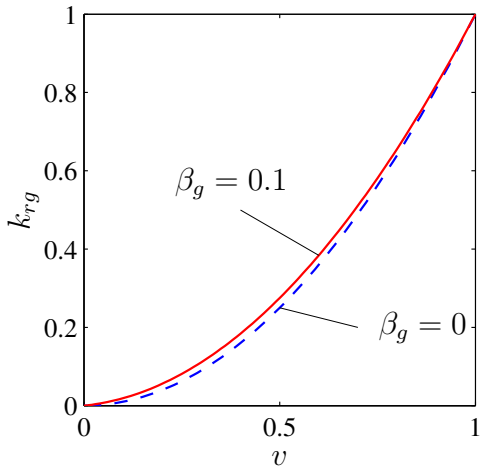

Figure 5. Relative permeability of gas as a function of its own saturation for two different values of the endpoint-slope: $\beta_g = 0$ and $\beta_g = 0.1$.

elliptic region take the form:

$$\begin{aligned} \nu_1 &= \Re\nu - i\Im\nu, \\ \nu_2 &= \Re\nu + i\Im\nu, \end{aligned} \tag{61}$$

where $\Re$ and $\Im$ indicate the real and imaginary part, respectively. Because outside an elliptic region eigenvalues are real and distinct, and inside they are complex conjugates, an elliptic region must be bounded by a curve along which eigenvalues are real and equal. This observation suggests using the quantity

$$\delta := (\nu_2 - \nu_1)^2 \tag{62}$$

to locate elliptic regions. The discriminant δ is positive for saturation states where the system is strictly hyperbolic, and negative where the system is elliptic. Therefore, elliptic regions are sets where $\delta < 0$, bounded by a contour $\delta = 0$. Figure 7 shows a contour plot of the discriminant δ on the entire ternary diagram for the two values of β_g. Both plots are quite similar except near the OW edge, that is, the states of low reduced gas saturation. The contour plot for the case $\beta_g = 0$ —Figure 7(a)— shows a strip near the OW edge where the discriminant attains local minima. This range was explored for elliptic regions. Only one elliptic region was found, located inside the small triangle marked in the figure. On the other hand, no elliptic regions are present in the case $\beta_g = 0.1$ —Figure 7(b).

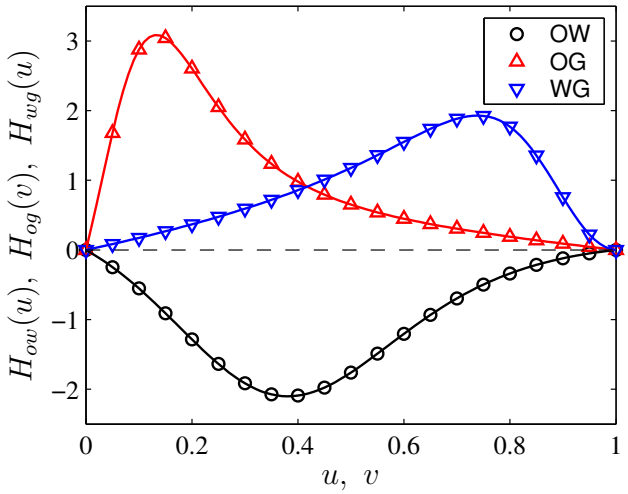

(a) $\beta_g = \beta_g^{\mathrm{ell}} = 0$

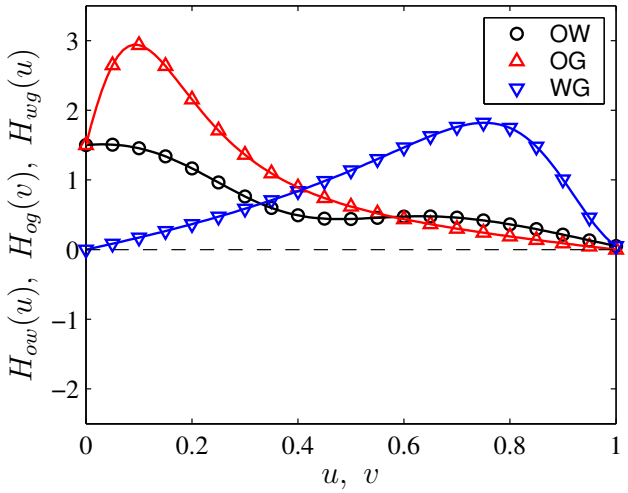

(b) $\beta_g = \beta_g^{\mathrm{hyp}} = 0.1$

Figure 6. Strict hyperbolicity on edges of the saturation triangle requires that all three functions $H_{ow}(u)$, $H_{og}(v)$, and $H_{wg}(u)$ are positive everywhere. This condition is: (a) violated when the value $\beta_g = 0$ is used; (b) satisfied when $\beta_g = 0.1$ is employed.

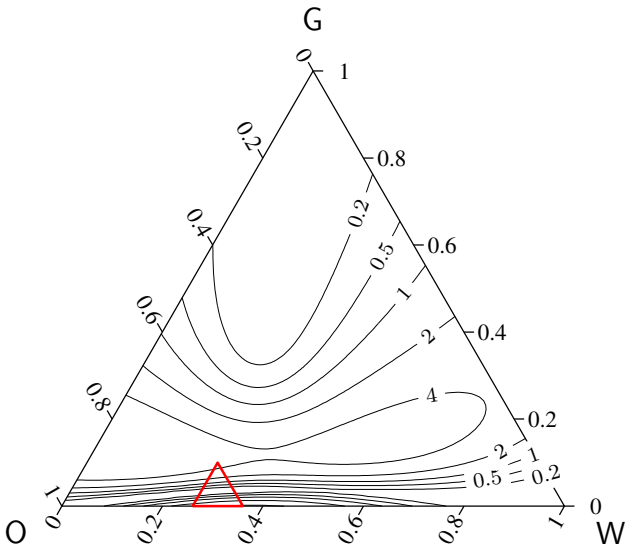

(a) $\beta_g = \beta_g^{\mathrm{ell}} = 0$

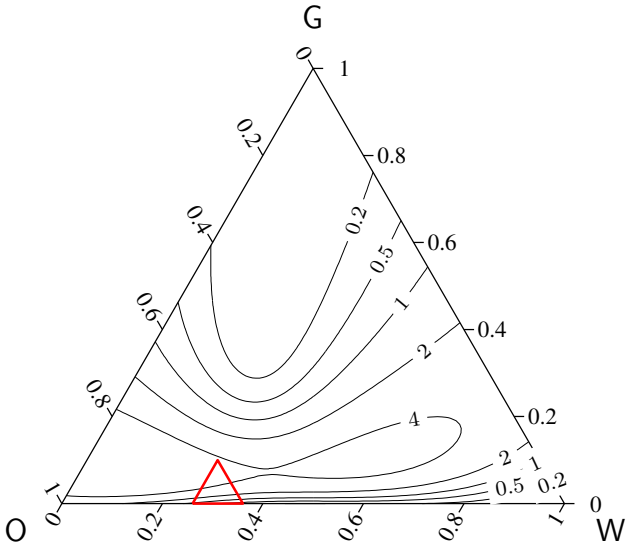

(b) $\beta_g = \beta_g^{\mathrm{hyp}} = 0.1$

Figure 7. Contour plot of the discriminant $\delta := (\nu_2 - \nu_1)^2$, evaluated on the saturation triangle for the simple relative permeability model (39)–(41) with: (a) $\beta_g = 0$; and (b) $\beta_g = 0.1$. The smaller triangle (△) denotes the zoomed area, detailed in Figure 8.

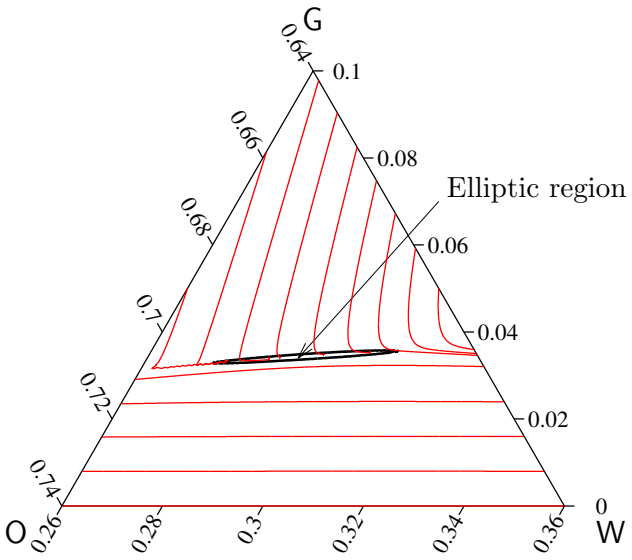

(a) $\beta_g = \beta_g^{\text{ell}} = 0$

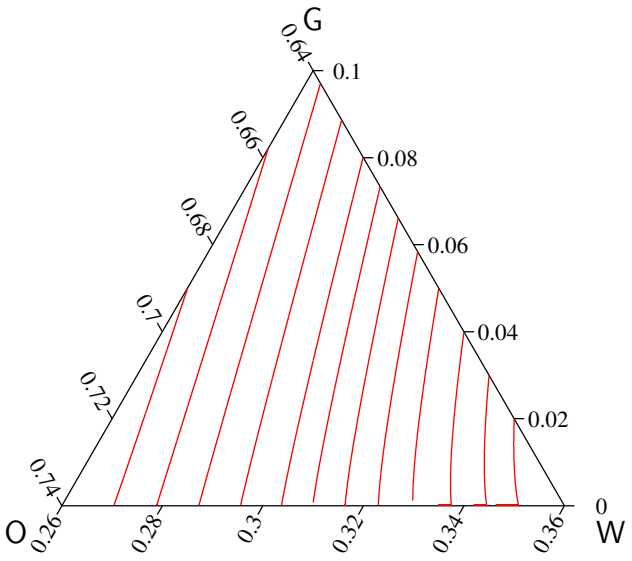

(b) $\beta_g = \beta_g^{\text{hyp}} = 0.1$

Figure 8. Fast characteristic paths evaluated on the small region indicated in Figure 7: (a) $\beta_g = 0$; and (b) $\beta_g = 0.1$. The presence of an elliptic region in (a) is accompanied by dramatic changes in the characteristic paths.

An i-characteristic path is an integral curve of the i-family, that is, a curve whose tangent at any saturation state is in the direction of the i-eigenvector $\boldsymbol{r}_i$. A detailed analysis of the characteristic paths was performed on the small saturation triangle indicated in Figure 7. For clarity, only the *fast* paths —corresponding to the 2-characteristic family— are shown in Figure 8. The most relevant feature is, of course, the presence of an elliptic region when $\beta_g = 0$. The elliptic region is very small in size, and located close to the edge of zero gas saturation. This is what is typically found [13,24,25,34] when using the most common relative permeability models. The presence of the elliptic region induces, however, a dramatic change of direction of the characteristic saturation paths —Figure 8(a). This feature is *not* restricted to the vicinity of the elliptic region but it propagates, rather, to the entire saturation triangle. In contrast, the saturation paths for the case $\beta_g = 0.1$ are smooth and slowly varying —Figure 8(b).

5 Conclusions

The main conclusion of this investigation is that it is possible to derive conditions that must be satisfied by the relative permeabilities, so that the system of equations governing one-dimensional three-phase flow with gravity is strictly hyperbolic. The essence is to acknowledge that a Darcy-like description of multiphase fluid flow is insufficient to capture all the multiscale features of multiphase flow. In this context, the relative permeabilities are left with the task of accounting for all the nonlinearity and unresolved physics of the problem. As a result, the relative permeabilities are *functionals*, which should depend not only on fluid saturations and saturation history, but also on the flow regime. They may, in principle, depend on the fluid viscosity ratios and the gravity number. This dependence, which is recognized in this investigation, helps elucidate why it is possible to develop strictly hyperbolic models of three-phase flow with gravity. The conditions that need to be imposed on the relative permeabilities may be justified from the point of view of the stability of displacements that take place in the porous medium. The analysis presented here is restricted to co-current *displacement* processes. In cases that involve mixed co-current and counter-current flow, capillarity effects cannot be dropped from the formulation.

We regard elliptic behavior —in otherwise hyperbolic models of three-phase flow— as an unintended artifact of an incomplete mathematical for-

mulation, rather than a necessary consequence dictated by physics [35]. We show, by means of an illustrative example, that elliptic regions induce a dramatic change in the characteristic saturation paths. We also show that compliance with the conditions for strict hyperbolicity derived in this paper may be achieved by a small modification of the relative permeability functions which is, nevertheless, sufficient to remove elliptic behavior.

The developments presented herein should serve as a motivation to: (1) employ sensible relative permeability models in traditional formulations of three-phase flow, (2) develop improved descriptions of multiphase flow in porous media, which supersede the straightforward extension of Darcy's equation, incorporate the inherent multiscale phenomena, and are still mathematically tractable.

ACKNOWLEDGEMENTS

This work was supported by the Laboratory Directed Research and Development Program of Lawrence Berkeley National Laboratory under the Department of Energy Contract No. DE-AC03-76SF00098. Funding provided by Barrié de la Maza, Jane Lewis, and Repsol-YPF fellowships, awarded to the first author, is also gratefully acknowledged.

References

[1] L. M. Abriola and G. F. Pinder. A multiphase approach to the modeling of porous media contamination by organic compounds, 1. Equation development. *Water Resour. Res.*, 21(1):11–18, 1985.

[2] L. M. Abriola and G. F. Pinder. A multiphase approach to the modeling of porous media contamination by organic compounds, 2. Numerical simulation. *Water Resour. Res.*, 21(1):19–26, 1985.

[3] A. E. Adenekan, T. W. Patzek, and K. Pruess. Modeling of multiphase transport of multicomponent organic contaminants and heat in the subsurface: Numerical-model formulation. *Water Resour. Res.*, 29(11):3727–3740, 1993.

[4] D. G. Avraam and A. C. Payatakes. Flow regimes and relative permeabilities during steady-state 2-phase flow in porous-media. *J. Fluid Mech.*, 293:207–236, 1995.

[5] D. G. Avraam and A. C. Payatakes. Generalized relative permeability coefficients during steady-state 2-phase flow in porous-media, and correlation with the flow mechanisms. *Transp. Porous Media*, 20(1–2):135–168, 1995.

[6] D. G. Avraam and A. C. Payatakes. Flow mechanisms, relative permeabilities, and coupling effects in steady-state two-phase flow through porous media. The case of strong wettability. *Ind. Eng. Chem. Res.*, 38(3):778–786, 1999.

[7] A. V. Azevedo and D. Marchesin. Multiple viscous profile Riemann solutions in mixed elliptic-hyperbolic models for flow in porous media. In B. L. Keyfitz and M. Shearer, editors, *Nonlinear Evolution Equations that Change Type*, volume 27 of *The IMA Volumes in Mathematics and its Applications*, pages 1–17. Springer-Verlag, New York, 1990.

[8] A. V. Azevedo and D. Marchesin. Multiple viscous solutions for systems of conservation laws. *Trans. Amer. Math. Soc.*, 347(8):3061–3077, 1995.

[9] K. Aziz and A. Settari. *Petroleum Reservoir Simulation*. Elsevier, London, 1979.

[10] G. I. Barenblatt. Micromechanics of fracture. In S.R. Bodner, J. Singer, A. Solan, and Z. Hashin, editors, *Proceedings of the XVIII International Congress on Theoretical and Applied Mechanics*, pages 25–52. Elsevier, Amsterdam, 1993.

[11] G. I. Barenblatt, V. M. Entov, and V. M. Ryzhik. *Theory of Fluid Flows through Natural Rocks*, volume 3 of *Theory and Applications of Transport in Porous Media*. Kluwer, Dordrecht, 1990. Expanded and revised edition of the original in Russian *Dvizhenie zhidkostei i gazov v prirodnykh plastakh*, Nedra Publishers, 1984.

[12] J. Bear. *Dynamics of Fluids in Porous Media*. Environmental Science Series. Elsevier, New York, 1972. Reprinted with corrections, Dover, New York, 1988.

[13] J. B. Bell, J. A. Trangenstein, and G. R. Shubin. Conservation laws of mixed type describing three-phase flow in porous media. *SIAM J. Appl. Math.*, 46(6):1000–1017, 1986.

[14] S. E. Buckley and M. C. Leverett. Mechanism of fluid displacement in sands. *Petrol. Trans.* AIME, 146:107–116, 1942.

[15] G. Chavent and J. Jaffré. *Mathematical Models and Finite Elements for Reservoir Simulation*, volume 17 of *Studies in Mathematics and its Applications*. Elsevier, North-Holland, 1986.

[16] K. H. Coats. Reservoir simulation: state of the art. *JPT*, 34(8):1633–1642, August 1982.

[17] A. H. Falls and W. M. Schulte. Features of three component, three phase displacement in porous media. *SPERE*, 7(4):426–432, November 1992.

[18] A. H. Falls and W. M. Schulte. Theory of three component, three phase displacement in porous media. *SPERE*, 7(3):377–384, August 1992.

[19] R. W. Falta, K. Pruess, I. Javandel, and P. A. Witherspoon. Numerical modeling of steam injection for the removal of nonaqueous phase liquids from the subsurface, 1. Numerical formulation. *Water Resour. Res.*, 28(2):433–449, 1992.

[20] R. W. Falta, K. Pruess, I. Javandel, and P. A. Witherspoon. Numerical modeling of steam injection for the removal of nonaqueous phase liquids from the subsurface, 1. Code validation and application. *Water Resour. Res.*, 28(2):451–465, 1992.

[21] F. J. Fayers. Extension of Stone's method I and conditions for real characteristics in three-phase flow. In *SPE 62nd Annual Technical Conference and Exhibition*, Dallas, TX, September 27–30, 1987. (SPE 16965).

[22] F. J. Fayers and J. W. Sheldon. The effect of capillary pressure and gravity on two-phase fluid flow in a porous medium. *Petrol. Trans.* AIME, 216:147–155, 1959.

[23] W. G. Gray and S. M. Hassanizadeh. Macroscale continuum mechanics for multiphase porous-media flow including phases, interfaces, common lines and common points. *Adv. Water Resour.*, 21:261–281, 1998.

[24] R. E. Guzmán and F. J. Fayers. Mathematical properties of three-phase flow equations. *SPEJ*, 2(3):291–300, September 1997.

[25] R. E. Guzmán and F. J. Fayers. Solution to the three-phase Buckley-Leverett problem. *SPEJ*, 2(3):301–311, September 1997.

[26] S. M. Hassanizadeh. Derivation of basic equations of mass transport in porous media, Part 2. Generalized Darcy's and Fick's laws. *Adv. Water Resour.*, 9:207–222, 1986.

[27] S. M. Hassanizadeh and W. G. Gray. Mechanics and thermodynamics of multiphase flow in porous media including interphase boundaries. *Adv. Water Resour.*, 13(4):169–186, 1990.

[28] S. M. Hassanizadeh and W. G. Gray. Toward an improved description of the physics of two-phase flow. *Adv. Water Resour.*, 16(1):53–67, 1993.

[29] H. Holden. On the Riemann problem for a prototype of a mixed type conservation law. *Comm. Pure Appl. Math.*, 40(2):229–264, 1987.

[30] H. Holden and L. Holden. On the Riemann problem for a prototype of a mixed type conservation law, II. In W. B. Lindquist, editor, *Current Progress in Hyperbolic Systems: Riemann Problems and Computations*, volume 100 of *Contemporary Mathematics*, pages 331–367. American Mathematical Society, Providence, RI, 1989.

[31] H. Holden, L. Holden, and N. H. Risebro. Some qualitative properties of 2×2 systems of conservation laws of mixed type. In B. L. Keyfitz and M. Shearer, editors, *Nonlinear Evolution Equations that Change Type*, volume 27 of *The IMA Volumes in Mathematics and its Applications*, pages 67–78. Springer-Verlag, New York, 1990.

[32] L. Holden. On the strict hyperbolicity of the Buckley-Leverett equations for three-phase flow in a porous medium. *SIAM J. Appl. Math.*, 50(3):667–682, 1990.

[33] M. D. Jackson and M. J. Blunt. Elliptic regions and stable solutions for three-phase flow in porous media. *Transp. Porous Media*, 48:249–269, 2002.

[34] P. J. Hicks Jr. and A. S. Grader. Simulation of three-phase displacement experiments. *Transp. Porous Media*, 24:221–245, 1996.

[35] R. Juanes and T. W. Patzek. Relative permeabilities for strictly hyperbolic models of three-phase flow in porous media. *Transp. Porous Media*, 2002. (Submitted).

[36] S. A. Kahn, G. A. Pope, and J. A. Trangenstein. Micellar/polymer physical property models for contaminant cleanup problems and enhanced oil recovery. *Transp. Porous Media*, 24(1):35–79, 1996.

[37] B. L. Keyfitz and M. Shearer, editors. *Nonlinear Evolution Equations that Change Type*, volume 27 of *The IMA Volumes in Mathematics and its Applications*. Springer-Verlag, New York, 1990.

[38] L. W. Lake. *Enhanced Oil Recovery*. Prentice-Hall, Englewood Cliffs, NJ, 1989.

[39] R. Lenormand. Pattern growth and fluid displacements through porous media. *Physica A*, 140:114–123, 1986.

[40] R. Lenormand, E. Touboul, and C. Zarcone. Numerical models and experiments on immiscible displacements in porous media. *J. Fluid Mech.*, 189:165–187, 1988.

[41] M. C. Leverett and W. B. Lewis. Steady flow of gas-oil-water mixtures through unconsolidated sands. *Petrol. Trans.* AIME, 142:107–116, 1941.

[42] W. B. Lindquist, editor. *Current Progress in Hyperbolic Systems: Riemann Problems and Computations*, volume 100 of *Contemporary Mathematics*. American Mathematical Society, Providence, RI, 1989.

[43] D. Marchesin and H. B. Medeiros. A note on the stability of eigenvalue degeneracy in nonlinear conservation laws of multiphase flow. In W. B. Lindquist, editor, *Current Progress in Hyperbolic Systems: Riemann Problems and Computations*, volume 100 of *Contemporary Mathematics*, pages 215–224. American Mathematical Society, Providence, RI, 1989.

[44] C. T. Miller, G. Christakos, P. T. Imhoff, J. F. McBride, J. A. Pedit, and J. A. Trangenstein. Multiphase flow and transport modeling in heterogeneous porous media: challenges and approaches. *Adv. Water Resour.*, 21(2):77–120, 1998.

[45] M. Muskat. *Physical Principles of Oil Production*. McGraw-Hill, New York, 1949.

[46] M. Muskat and M. W. Meres. The flow of heterogeneous fluids through porous media. *Physics*, 7:346–363, 1936.

[47] D. W. Peaceman. *Fundamentals of Numerical Reservoir Simulation*, volume 6 of *Developments in Petroleum Science*. Elsevier, Amsterdam, 1977.

[48] G. A. Pope. The application of fractional flow theory to enhanced oil recovery. *SPEJ*, 20(3):191–205, June 1980. *Petrol. Trans.* AIME, 269.

[49] L. A. Rapoport and W. J. Leas. Properties of linear waterfloods. *Petrol. Trans.* AIME, 198:139–148, 1953.

[50] L. A. Richards. Capillary conduction of liquids through porous mediums. *Physics*, 1:318–333, 1931.

[51] D. G. Schaeffer and M. Shearer. The classification of 2×2 systems of nonstrictly hyperbolic conservation laws, with application to oil recovery. *Comm. Pure Appl. Math.*, 40(1):141–178, 1987. Appendix with D. Marchesin and P. J. Paes-Leme.

[52] M. Shearer. Loss of strict hyperbolicity of the Buckley-Leverett equations for three phase flow in a porous medium. In M. F. Wheeler, editor, *Numerical Simulation in Oil Recovery*, volume 11 of *The IMA Volumes in Mathematics and its Applications*, pages 263–283. Springer-Verlag, New York, 1988.

[53] M. Shearer and J. A. Trangenstein. Loss of real characteristics for models of three-phase flow in a porous medium. *Transp. Porous Media*, 4:499–525, 1989.

[54] D. Silin and T. Patzek. On the Barenblatt model of spontaneous countercurrent imbibition. *Transp. Porous Media*, 2002. (Submitted).

[55] H. L. Stone. Probability model for estimating three-phase relative permeability. *JPT*, 23(2):214–218, February 1970. *Petrol. Trans.* AIME, 249.

[56] H. L. Stone. Estimation of three-phase relative permeability and residual oil data. *J. Can. Petrol. Technol.*, 12(4):53–61, 1973.

[57] J. A. Trangenstein. Three-phase flow with gravity. In W. B. Lindquist, editor, *Current Progress in Hyperbolic Systems: Riemann Problems and Computations*, volume 100 of *Contemporary Mathematics*, pages 147–159. American Mathematical Society, Providence, RI, 1989.

[58] M. S. Valavanides, G. N. Constantinides, and A. C. Payatakes. Mechanistic model of steady-state two-phase flow in porous media based on ganglion dynamics. *Transp. Porous Media*, 30(3):267–299, 1998.

[59] Y. C. Yortsos, B. Xu, and D. Salin. Delineation of microscale regimes of fully-developed drainage and implications for continuum models. *Comput. Geosci.*, 5(3):257–278, 2001.

[60] Y. Zhang, M. Shariati, and Y. C. Yortsos. The spreading of immiscible fluids in porous media under the influence of gravity. *Transp. Porous Media*, 38(1–2):117–140, 2000.